JOURNAL OF MATERIALS SCIENCE 20 (1985) 4377–4386

The mechanical behaviour of PVC short-fibre composites

J. YUAN, A. HILTNER, E. BAER
Department of Macromolecular Science, Case Institute of Technology, Case Western Reserve University, Cleveland, Ohio 44106, USA

D. RAHRIG
BF Goodrich Research Center, Brecksville, Ohio 44141, USA

Competitive deformation processes between interfacial "debonding" and matrix cracking at the fibre ends is shown for the short-fibre reinforced composites of polyvinyl chloride (PVC). The increase of interfacial shear strength by chemical coupling prevents early failure at the interface, thus increasing the tensile failure stress of short-fibre composites. The previously proposed general yield criterion for PVC and its short-fibre composites is also examined. No significant effect due to improved fibre–matrix adhesion on the upper shear yielding of short-fibre composites is observed. The matrix flow in the post-yield region is less restricted when debonding occurs.

1. Introduction

The mechanics and properties of discontinuous fibre-reinforced composites have been extensively studied during the past few decades. Theoretical calculations indicate that, when a fibre composite is stressed, very high shear stresses occur at the interface between matrix and fibre [1–3]. Photoelastic experiments show that these interfacial shear stresses are even higher than the theories suggest, especially at the fibre ends [4]. Recently, Piggot [5] reported that the mechanical properties of short-fibre reinforced composites depend upon the interface as much as on the properties of fibre and matrix. Furthermore, Sato *et al.* [6] demonstrated from scanning electron microscope (SEM) observations that interfacial "debonding" occurs prior to the failure of short-fibre reinforced polyamide thermoplastics. In a previous study [7] we have observed three types of deformation behaviour in the short glass-fibre reinforced composites of polyvinyl chloride (PVC) under superimposed hydrostatic pressure. Competitive pressure-dependent failure processes in the composites are strongly affected by debonding at the fibre–matrix interface. The purpose of this work was to study the effects of interfacial adhesion on these pressure-dependent deformation processes. The previously proposed general yield criterion for PVC and its short-fibre composites was also examined.

2. Experimental details

2.1. Materials

The materials used in this study were PVC and its short glass-fibre reinforced composites, supplied by the BF Goodrich Company. The PVC compound was prepared from Geon 110X346 PVC resin ($M_w = 1.0 \times 10^5$, $M_w/M_n = 2.7$) with two parts of Thermolite 31 stabilizer (dibutyl tin bisisooctyl thioglycolate) and one-half part of 629A oxidized polyethylene supplied by Allied Corporation, which serves as a processing lubricant.

The poorly coupled, glass-fibre reinforced PVC composites were prepared using as received PPG 3130 $\frac{1}{4}$in. (6 mm) chopped glass strands. The PVC composites with good fibre–matrix adhesion were prepared using a BFG proprietary coupling technology and $\frac{1}{4}$in. E-glass fibres.

0022–2461/85 $03.00 + .12

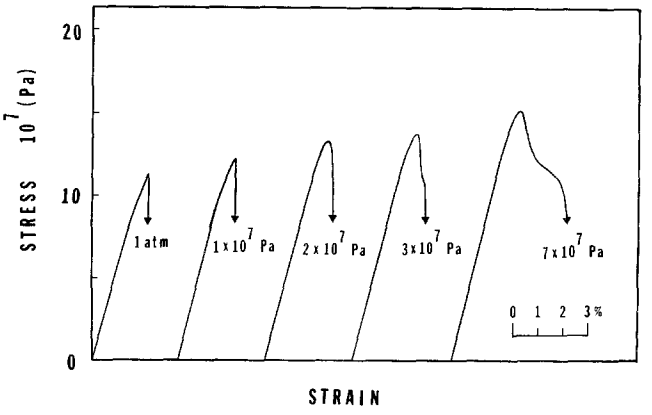

Figure 1 Stress–strain curves of well-coupled 20 wt % short glass-fibre reinforced PVC at various pressures.

The poorly coupled composites were mixed on a twin screw extruder and pelletized. The well-coupled composites were Banbury mixed, milled to sheet on a 6 in. × 12 in. (152 mm × 305 mm) differential speed two-roll mill, and then granulated. The poorly coupled pellets and the well-coupled granules were then injection moulded into cylindrical tensile specimens described in a previous publication [7], which produced a preferred fibre orientation along the gauge section. The glass loadings used in this study were 20% and 30% by weight.

2.2. Tensile measurements

A constant cross-head speed testing machine which contains silicone oil (Dow Corning 200 fluid, 500 c st ($5\,m^2\,sec^{-1}$)) as pressure-transmitting fluid was used in this study of tensile behaviour under superimposed hydrostatic pressure. In order to prevent possible environmental effects due to the pressure-transmitting fluid, the gauge section of test specimens was sealed with Teflon tape and silicon rubber. Tensile measurements of sealed specimens were conducted at a strain rate of approximately $10\%\,min^{-1}$ at room temperature. Tensile measurements at atmospheric pressure were performed in an Instron testing machine.

2.3. Scanning electron microscopy

A three-point bending technique described by Sato *et al.* [6] was used to study the irreversible deformation processes of short-fibre reinforced composites. The sample stage of the SEM was modified so that the three-point bending tests could be performed on the stage. The gauge section of tensile specimens was polished to 1.5 mm thickness using 0.05 μm alumina powders. The tensile surface was coated with platinum for SEM observation. The observation was focused on the region under maximum deflection.

The fracture surfaces of tensile specimens fractured at various pressures were also examined using an SEM. Samples were decorated with platinum before observation.

3. Results and discussion

3.1. Stress and strain behaviour

Tensile measurements under hydrostatic pressure of sheathed specimens were performed for PVC and its short glass-fibre reinforced composites at pressures from atmospheric pressure to 3.0×10^8 Pa. Fig. 1 shows the nominal tensile stress–strain curves of the well-coupled 20 wt % glass-fibre reinforced composites at various pressures. Typical brittle-fracture behaviour was observed up to 1×10^7 Pa. At and above 2×10^7 Pa an upper shear yielding was observed. The yield stress and fracture strain increase as the hydrostatic pressure increases. A similar pressure effect on the tensile stress and strain behaviour was also observed for well-coupled 30 wt % short-fibre composites as shown in Fig. 2. Tensile brittle-fracture behaviour could be observed up to 4×10^7 Pa. The brittle fracture stress increases significantly with increasing pressure. At and above 5×10^7 Pa an upper shear yielding occurred prior to sample fracture. The yield stress and fracture strain also increase with pressure. Fig. 3 shows the gauge section of test specimens of 30 wt % glass-fibre reinforced composites fractured at various pressures. Note that samples fracture at 90° to the axis of tensile stress at pressures from atmospheric pressure to 4×10^7 Pa. The transition from tensile to shear fracture occurred at a pressure between 4×10^7 and 5×10^7 Pa. At and above 5×10^7 Pa,

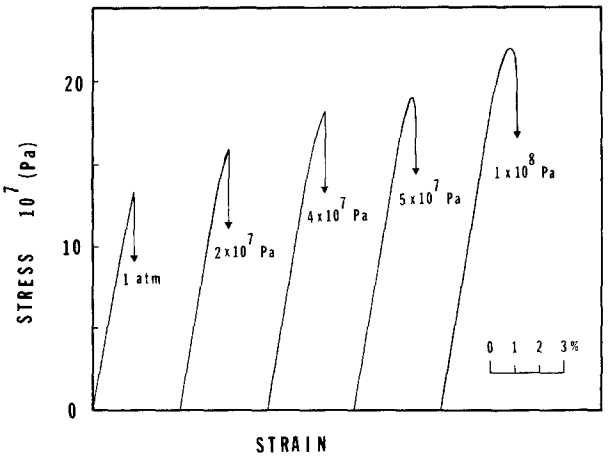

Figure 2 Stress–strain curves of well-coupled 30 wt % short glass-fibre reinforced PVC at various pressures.

samples fractured in shear as indicated by approximate 45° to the first principal stress axis.

Fig. 4 shows the principal maximum stress of PVC and its short glass-fibre reinforced composites at various pressures, where the principal tensile stress is equal to tensile stress minus pressure. It is noted that the principal tensile brittle fracture stress is independent of hydrostatic pressure. The principal upper yield stress decreases with increasing pressure. The transition from tensile brittle fracture to upper shear yielding occurs when the brittle fracture stress and upper yield stress curves intersect, suggesting that this transition is controlled by these

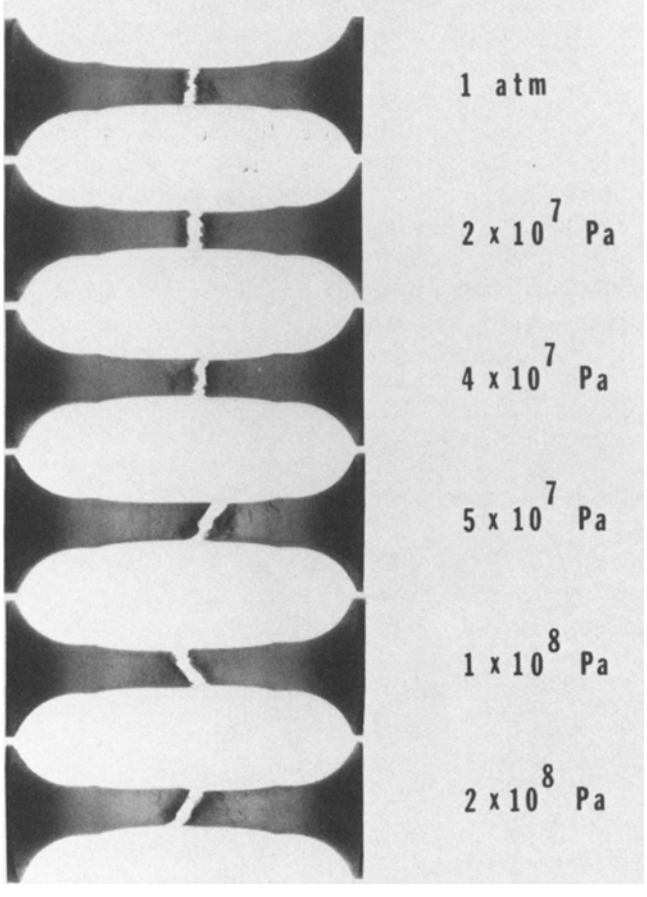

Figure 3 The gauge section of tensile specimens for well-coupled 30 wt % glass-fibre reinforced PVC fractured at various pressures.

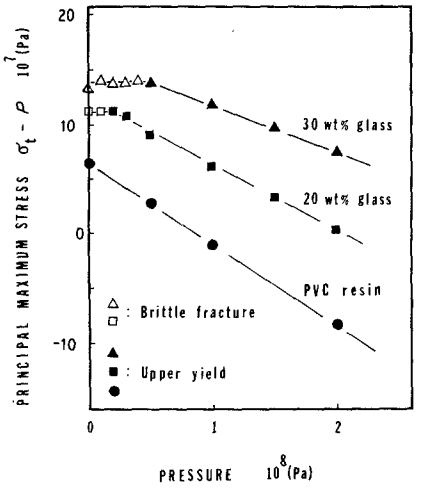

Figure 4 Principal maximum stress of PVC and its well-coupled short-fibre reinforced composites at various pressures.

competitive processes of dilational and shearing flow. Furthermore, both the brittle fracture stress and upper yield stress increase with fibre loading, and the transition pressure increases as fibre loading increases.

In Fig. 5, the effect of fibre–matrix adhesion is shown by comparison of the data for the well-coupled 30 wt % glass-fibre reinforced sample (Fig. 2) with data for a composite with poor coupling taken from Yuan *et al.* [7]. Typical brittle-fracture behaviour is observed at pressures from atmospheric pressure to 4×10^7 Pa for both well-coupled and poorly coupled systems. The fracture stress and fracture strain are increased by improved fibre–matrix adhesion. At 5×10^7 Pa an upper shear yielding occurs for the well-coupled composite, while for the poorly coupled composite a Type II deformation behaviour, which shows a sharp drop in stress due to interfacial debonding followed by matrix shear yielding, is observed. At and above 1.0×10^8 Pa, the upper shear yielding occurs for both well-coupled and poorly coupled systems. No significant effect due to coupling agent on the upper yield stress is observed. The fracture strain of poorly coupled composites is higher than that of the well-coupled composites.

A composite plot of principal maximum stress for both well-coupled and poorly coupled 30 wt % glass-fibre reinforced composites is shown in Fig. 6. It is noted that the principal tensile failure stress is independent of hydrostatic pressure for the well-coupled and poorly coupled systems. The principal brittle fracture stress increases by about 15% due to the increase of interfacial adhesion at the fibre–matrix interface in the well-coupled system. On the other hand, the principal upper shear yield stress decreases as pressure increases. No significant effects due to interfacial adhesion on the upper shear yield stress of short-fibre composites was observed. The absence of Type II deformation behaviour for the composites with good coupling is attributed to the increase of interfacial shear strength which prevents sample failure at the interface between glass fibre and matrix.

3.2. Deformation processes

In order to visualize the irreversible deformation processes of short-fibre composites, a three-point bending technique described by Sato *et al.*

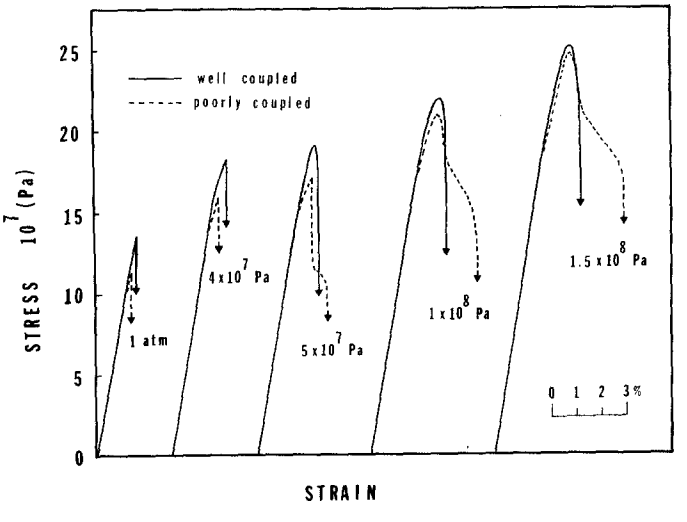

Figure 5 Stress–strain curves of well coupled and poorly coupled 30 wt % short-fibre reinforced composites at various pressures.

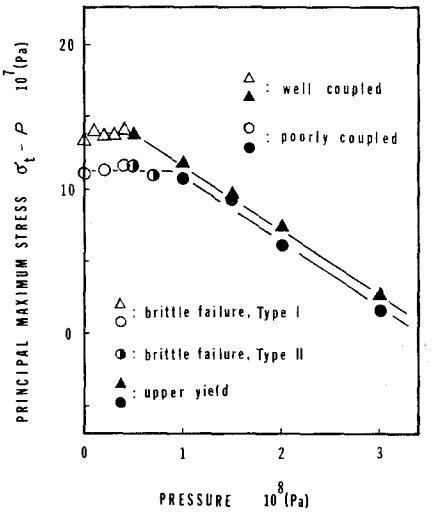

Figure 6 Principal maximum stress of well-coupled and poorly coupled 30 wt % short-fibre reinforced PVC.

[6] was utilized for SEM observation. The gauge section of tensile specimens was polished using 0.05 μm alumina powders. The surface of as-polished specimens is shown in Fig. 7. Fibres are embedded in the matrix. Samples were mounted so that the direction of preferential fibre orientation was in the direction of tensile stress. Fig. 8 shows the deformation process of well-coupled 30 wt % glass-fibre reinforced composite at atmospheric pressure. Arrows indicate the direction of tensile stress. Figs. 8a and b show crack initiation at the fibre ends when the composite is stressed. These fibre-end cracks become more numerous in the region of maximum stress as the level of strain increases. When the stress further increases, fibre-end cracks propagate into the matrix as shown in Fig. 8c. These propagating cracks either join each other to form a larger crack (Fig. 8d), or interact with neighboring fibres to cause interfacial debonding as shown in Fig. 8e.

The typical brittle tensile fracture surface of well-coupled short-fibre composites is shown in Fig. 9. Strong adhesion at the fibre–matrix interface was observed. Fibre ends were also observed on the fracture surface which are believed to be the sites of crack initiation. At higher magnification void formation was observed in the matrix near fibre ends (Fig. 10). This indicates that crack propagation was preceded by matrix voiding. This matrix voiding was suppressed by the superimposed hydrostatic pressure. Fig. 11 shows the fracture surface of well-coupled 30 wt % short-fibre composites fractured at a higher pressure of 2×10^7 Pa. Numerous elongated fibrils were observed in the matrix near fibre ends. The diameter of these elongated fibrils is about 0.1 μm, which is about the same size as the craze fibrils of PVC reported by Schinker, Konczol and Doll [8] from fatigue test.

Fig. 12 shows the irreversible deformation process of poorly coupled 30 wt % short glass-fibre reinforced composite at the fibre–matrix interface at atmospheric pressure. Arrows indicate the direction of tensile stress in the three-point bending experiment. Again cracks initiate at fibre ends when the short-fibre composite is stressed as shown in Fig. 12a. As the level of strain further increases, these fibre-end cracks propagate along the interface between fibre and matrix (Fig. 12b). No propagation of fibre-end cracks into the matrix (as shown in Fig. 8c) is observed for the poorly coupled composites. It is suggested that the high stress concentration at fibre-end crack tips was reduced by interfacial debonding. In Fig. 13, the typical brittle tensile fracture surface of short-fibre composites with poor coupling is shown. Debonding was observed at the fibre–matrix interface.

Fig. 14 illustrates the competitive tensile failure processes for uniaxially oriented short-fibre reinforced composites. When the tensile stress is increased, cracks initiate at fibre ends. These fibre-end cracks propagate into the matrix as the maximum tensile stress at the crack tips reaches the critical tensile stress of the matrix, where the critical tensile stress σ_{11}^{crit} is a material constant of the matrix. On the other hand, it is known that

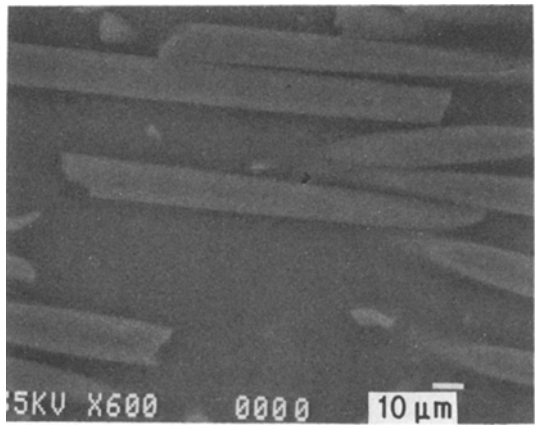

Figure 7 Scanning electron micrograph of the surface of an as-polished specimen.

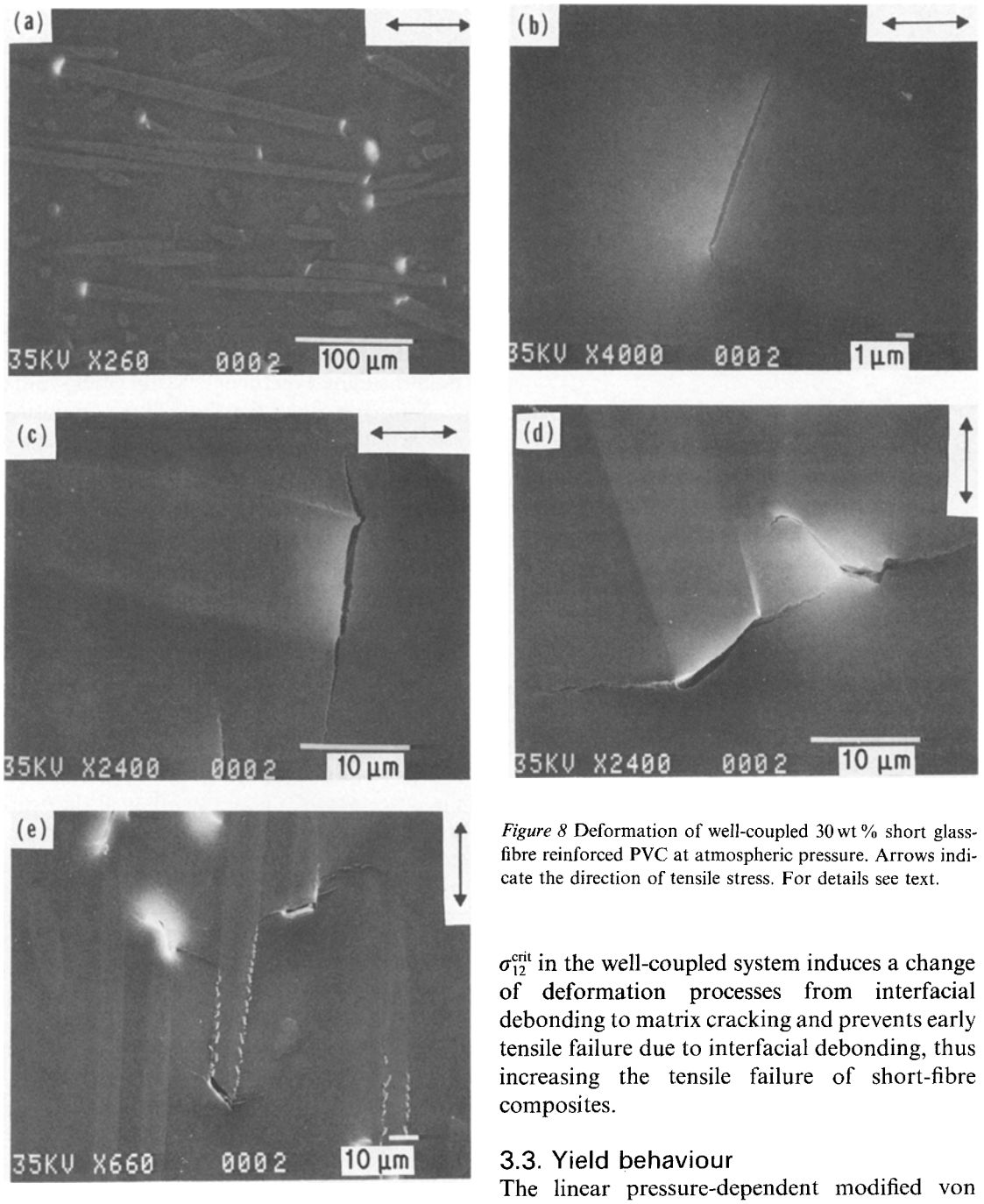

Figure 8 Deformation of well-coupled 30 wt % short glass-fibre reinforced PVC at atmospheric pressure. Arrows indicate the direction of tensile stress. For details see text.

very high shear stresses occur at the fibre–matrix interface especially near fibre ends when a short-fibre composite is stressed [4]. As the maximum shear stress at fibre ends reaches the critical interfacial shear stress σ_{12}^{crit}, the fibre-end cracks propagate along the interface between fibre and matrix. In the poorly coupled system σ_{12}^{crit} is reached before σ_{11}^{crit} and interfacial debonding occurs. The increase of interfacial shear strength σ_{12}^{crit} in the well-coupled system induces a change of deformation processes from interfacial debonding to matrix cracking and prevents early tensile failure due to interfacial debonding, thus increasing the tensile failure of short-fibre composites.

3.3. Yield behaviour

The linear pressure-dependent modified von Mises yield criterion [9–13] which successfully describes the yield stress of polymers is not adequate for fibre-reinforced composite systems. We have previously shown that in order to describe the yield behaviour of short-fibre reinforced PVC, one has to take into account both the heterogeneity and possible anisotropy in the composite system. Thus, the von Mises yield criterion should be written in a more general form as follows [7, 14]:

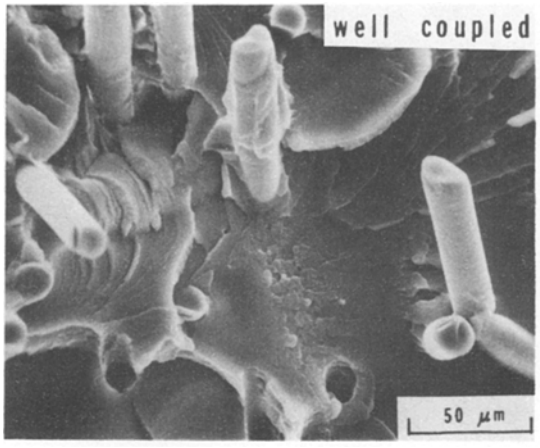

Figure 9 Scanning electron micrograph of the fracture surface of well-coupled 20 wt % short glass-fibre reinforced PVC fractured at atmospheric pressure.

$$\tau'_{oct} + \mu\sigma_{oct} = K_{oct}$$

where

$$\tau'_{oct} = 1/3\,[K_{12}^2(\sigma_1 - \sigma_2)^2 + K_{23}^2(\sigma_2 - \sigma_3)^2 + K_{31}^2(\sigma_3 - \sigma_1)^2]^{1/2}$$

is the octahedral shear stress responsible for the shear yielding, $\sigma_{oct} = 1/3\,(\sigma_1 + \sigma_2 + \sigma_3)$ is the octahedral normal stress, and K_{oct} and μ (the octrahedral normal stress coefficient) are material constants of the matrix. The material constants K_{12}, K_{23} and K_{31} are a function of fibre orientation and fibre loading. In the case of random fibre orientation $K_{12} = K_{23} = K_{31}$. For virgin PVC, $K_{12} = K_{23} = K_{31} = 1$. In our experimental conditions, $\sigma_1 = \sigma_t - P$ and $\sigma_2 = \sigma_3 = -P$. Due to cylindrical symmetry in the test specimens, $K_{12} = K_{31}$. The value of K_{12} can then be obtained as the ratio of tensile yield stress of PVC to that of the composites at zero octahedral normal stress.

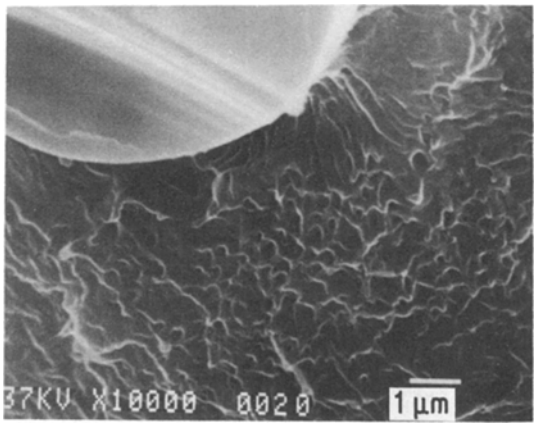

Figure 10 Scanning electron micrograph of the fracture surface of well-coupled 30 wt % short glass-fibre reinforced PVC fractured at atmospheric pressure.

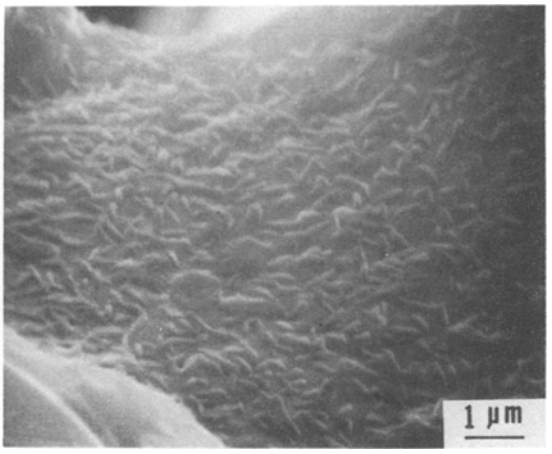

Figure 11 Scanning electron micrograph of the fracture surface of well-coupled 30 wt % short-fibre composites fractured at 2×10^7 Pa.

The plot of the octahedral shear stress, τ'_{oct}, and the octahedral normal stress corresponding to the upper shear yielding of PVC and the short-fibre composites is shown in Fig. 15. It is noted that this form of the von Mises yield criterion fits our experimental data for both PVC and the composites. All data points fall on the same line. The values calculated from the best linear least-squares fit of the data are $\mu = 0.11$ and $K_{oct} = 3.3 \times 10^7$ Pa, which agree with the previous studies of the yield behaviour of PVC [9, 15]. This indicates that the upper shear yielding behaviour of the short glass-fibre reinforced composites is controlled by the bulk yielding of the matrix (PVC). Fig. 16 shows the fracture surface of the well-coupled, 30 wt % short-fibre composite fractured at 5×10^7 Pa, where the sample fractured right after the upper yield. It is noted that the matrix fractured in a ductile shear manner.

In Fig. 17, the reinforcement factor of upper shear yielding for both well-coupled and poorly coupled short glass-fibre reinforced composites is shown. The reinforcement factor $1/K_{12}$ increases linearly with the volume fraction of glass fibre in the composites at least up to 20 vol %. This indicates that bulk yielding of the matrix is constrained by adjacent glass fibres. However, no significant effects due to interfacial adhesion on the upper shear yielding of the composites is observed.

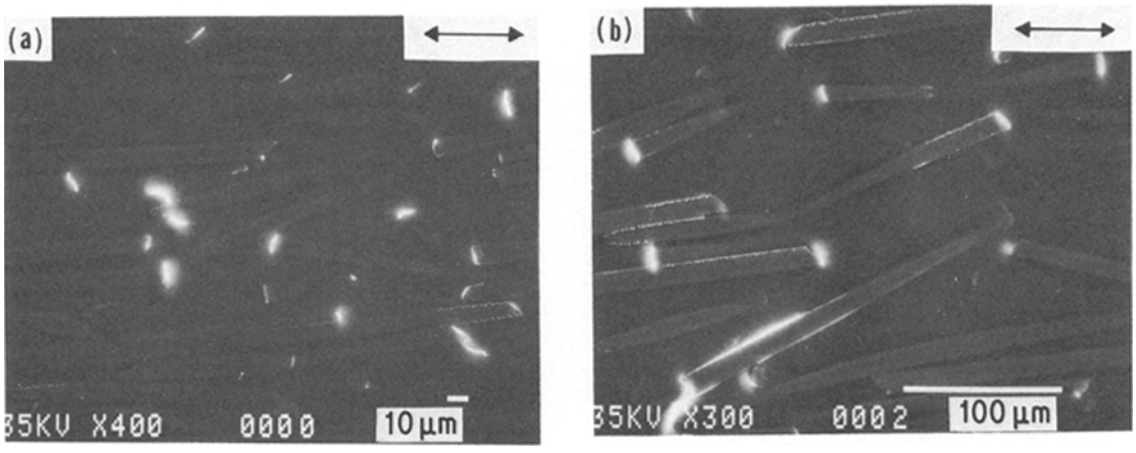

Figure 12 Deformation of poorly coupled 30 wt % short glass-fibre reinforced PVC at atmospheric pressure. Arrows indicate the direction of tensile stress.

Fig. 18 shows the fracture strain of 20 and 30 wt % short glass-fibre reinforced composites at various pressures, where samples fractured after the upper shear yielding. The fracture strain decreases as the fibre loading increases for the composites, both for well-coupled and poorly coupled interfaces. In part this is due to the restriction of matrix flow in the post-yield region by glass fibres in the composites. Interestingly, matrix flow is less restricted when debonding occurs and the fracture strain of poorly coupled composites is higher than that of the well-coupled composites.

4. Conclusions

(a) The brittle-fracture stress of short glass-fibre reinforced PVC increases as the adhesion at the fibre–matrix interface increases. Competitive deformation processes between interfacial debonding and matrix cracking at the fibre ends is proposed. The increase of interfacial shear strength by coupling prevents early failure at the

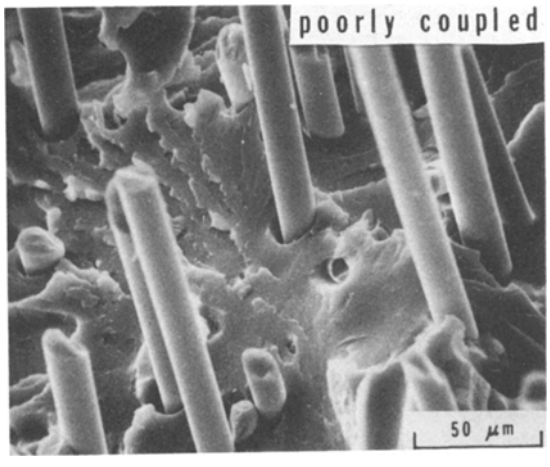

Figure 13 Scanning electron micrograph of the fracture surface of poorly coupled 20 wt % short-fibre composites reinforced PVC fractured at atmospheric pressure.

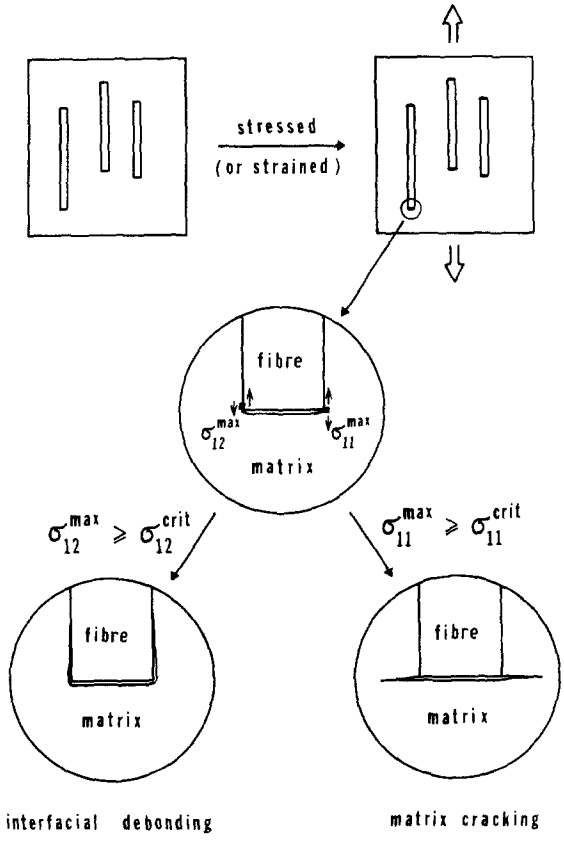

Figure 14 Schematic of deformation processes of uniaxially oriented short-fibre reinforced composites.

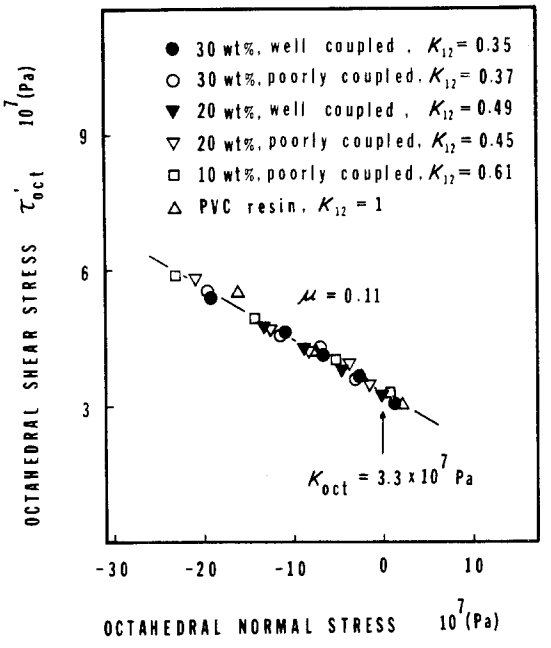

Figure 15 The upper shear yield stress of PVC and its short glass-fibre reinforced composites expressed as octahedral shear stress τ'_{oct} against octahedral normal stress.

interface, thus increasing the tensile failure stress of short-fibre composites.

(b) The Type II deformation behaviour, which shows a sharp drop in stress due to interfacial debonding followed by matrix yielding, is absent in the composites with good coupling at the fibre–matrix interface. The fracture strain after upper shear yielding is higher for the composites with poor coupling.

(c) No significant effects due to interfacial adhesion on the upper shear yield behaviour

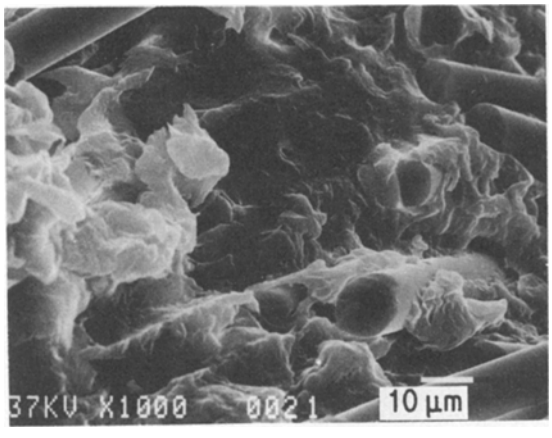

Figure 16 Scanning electron micrograph of the fracture surface of well-coupled 30 wt % short-fibre composites fractured at 5 × 10^7 Pa.

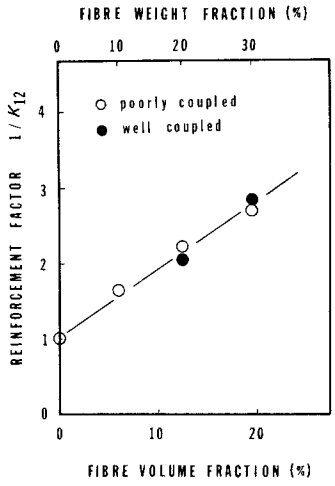

Figure 17 Reinforcement factor, K_{12}, corresponding to upper shear yielding of short glass-fibre reinforced PVC.

of short-fibre composites is observed. The reinforcement factor $1/K_{12}$ corresponding to upper shear yielding of short glass-fibre reinforced PVC increases linearly with the volume fraction of glass-fibre in the composites within the experimental range.

Acknowledgements

This work benefited from numerous stimulating discussions with Dr C. Carman. The generous financial support of the BF Goodrich Company and the National Science Foundation (grant ISI 8116103) through their cosponsorship of the Center for Applied Polymer Research is gratefully acknowledged.

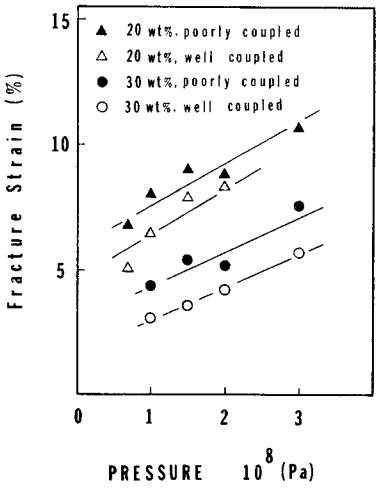

Figure 18 Fracture strain of short-fibre reinforced composites at pressures where samples fractured after upper shear yielding.

References

1. H. L. COX, *Br. J. Appl. Phys.* **3** (1952) 72.
2. B. W. ROSEN, in "Fiber Composite Materials" (American Society for Metals, Metals Park, Ohio, 1965) p. 37.
3. A. KELLY, "Strong Solids" (Clarendon, Oxford, 1966) p. 121.
4. W. R. TYSON and G. J. DAVIES, *Br. J. Appl. Phys.* **16** (1965) 199.
5. M. R. PIGGOTT, *Polym. Composites* **3** (1982) 179.
6. N. SATO, T. KURAUCHI, S. SATO and O. KAMIGAITO, *J. Mater. Sci. Lett.* **2** (1983) 188.
7. J. YUAN, A. HILTNER, E. BAER and D. RAHRIG, *Polym. Eng. Sci.* **24** (1984) 844.
8. M. G. SCHINKER, L. KONCZOL and W. DOLL, *J. Mater. Sci. Lett.* **1** (1982) 475.
9. J. JUAN, A. HILTNER and E. BAER, *J. Mater. Sci.* **18** (1983) 3063.
10. A. W. CHRISTIANSEN, E. BAER and S. V. RADCLIFFE, *Phil. Mag.* **24** (1971) 451.
11. S. S. STERNSTEIN and L. ONGCHIN, *ACS Polym. Prepr.* **10** (1969) 1117.
12. S. S. STERNSTEIN and F. A. MYERS, *J. Macromol. Sci. Phys.* **B8** (1973) 539.
13. A. NADAI, *J. Appl. Mech.* **1** (1933) 111.
14. J. YUAN, A. HILTNER, E. BAER and D. RAHRIG, Proceedings of Society of Plastics Engineers Annual Technical Conference, New Orleans, 1984 (SPE Inc., Brookfield Center, Connecticut) p. 672.
15. P. B. BOWDEN and J. A. JAKES, *J. Mater. Sci.* **7** (1972) 52.

Received 12 November
and accepted 18 December 1984